

1 **Title: A fine-grained behavior-based approach to estimating the probability of**
2 **collision between moving vehicles and birds**

Authors:

- 1) Ryan B. Lunn¹
- 2) Bradley F. Blackwell²
- 3) Esteban Fernández-Juricic¹

¹ Department of Biological Sciences, Purdue University, 915 Mitch Daniels Blvd, West Lafayette, IN, 47907, United States of America

² United States Department of Agriculture, Animal and Plant Health and Inspection Services, National Wildlife Research Center, Sandusky, 610 Columbus Ave, OH, 44870, United States of America

Corresponding Author: Ryan B. Lunn, email: rlunn@purdue.edu

3

Keywords: Road Ecology, Animal Behavior, Animal & Vehicle Collisions, Escape Behavior, Bird & Aircraft Collisions, Canada geese, Modeling, Drones

Open Research Statement

All code, files, supplementary material and data generated from this study are available at https://osf.io/9rh47/overview?view_only=1750d6840d3a4478bec0432b2fec2424

4 **Conflict of Interest:**

5 No conflict of interest declared

6

7 **Abstract**

8 1. Collisions between animals and vehicles contribute to biodiversity loss, threaten human
9 safety, and have economic consequences. Escape responses of wildlife to vehicles are a
10 critical factor in determining whether a collision occurs. However, presently species-

11 specific vulnerability estimates do not consider the species escape behavior, potentially
12 resulting in inaccurate mortality estimates.

13 2. Recently, a mathematical model was proposed to estimate whether a collision occurs
14 considering fine-grained properties of both an approaching vehicle and the species escape
15 response. Herein, we expanded upon an existing model and applied it for the first time to
16 estimate the probability of collision in a behavioral experiment where a UAS directly
17 approached Canada geese with different light (light-off, light-on steady, light-on pulsing)
18 and approach type (level, descending) treatments.

19 3. The probability of collision for the light-on steady and light-on pulsing treatment
20 increased by 9.92% and 25.47%, respectively, during level approaches but decreased
21 during descending approach treatments by 34.38% and 37.24%, respectively, relative to
22 the light-off treatment. We attribute this interaction effect to differences in the ratio of
23 UAS to LED light surface area.

24 4. We examined the role of the different parameters in the model and found that flight-
25 initiation distance had the largest effect size, followed by escape trajectory, and UAS
26 altitude. Specifically, longer flight-initiation distances, an increase in an away escape
27 trajectory, and higher UAS altitude all contributed to reducing the probability of collision.

28 5. *Synthesis and applications.* Using a fine-grained behavioral approach, our model can
29 provide estimates of the probability of an animal-vehicle collision when observing a
30 collision is either logistically challenging or unethical. We also demonstrate that our
31 model can provide quantitative guidance on UAS based hazing strategies to improve
32 animal welfare. Lastly, our model can be used to quantitatively estimate how many
33 animal-vehicle interactions were avoided due to the escape response of the animal, thus

34 enabling conservation strategies to not just focus on reducing collisions but also
35 promoting successful avoidance.

36 **Introduction**

37 Collisions between animals and vehicles regularly have lethal consequences for wildlife,
38 contributing to biodiversity loss (Loss et al., 2015, Lima et al., 2015, Grilo et al., 2021, Moore et
39 al., 2024), in addition to threatening human safety, and economic cost (Huijser et al., 2008,
40 Conover, 2019). A common practice to prevent animal-vehicle collisions is to exclude animals
41 from areas near transportation routes or infrastructure to reduce collisions by reducing the
42 probability of an animal and vehicle interaction (Glista et al., 2009, DeVault et al., 2013, van der
43 Ree et al., 2015, Rytwinski et al., 2016). However, such a drastic strategy is often not logistically
44 possible (Ascensão, et al., 2013, Huijser, et al., 2016, Spanowicz et al., 2020). Consequently,
45 other strategies have been used, such as hazing (Harris et al., 1998, Belant, 2011, Seiler &
46 Olsson, 2017), deterring wildlife from moving vehicles (Blackwell et al, 2012, Schoeman, et al.,
47 2020, Pakula et al., 2025) or adjusting vehicle trajectory (Mammeri et al., 2016, Silva &
48 Calabrese, 2024). One of the challenges of assessing different strategies has been the limited
49 theoretical frameworks to estimate the probability of collision between the vehicle and the
50 animal (Lunn et al., 2022).

51 The escape response of wildlife near an approaching vehicle is commonly invoked as a
52 critical factor in determining whether a collision does or does not occur (DeVault et al., 2015,
53 Blackwell et al., 2019, Brieger et al., 2022). Escape responses of prey animals to approaching
54 *predators* form a sequence of dynamic behaviors (Lima & Dill, 1990, Cooper & Blumstein,
55 2015, Evans et al., 2019, Branco & Redgrave, 2020), where multiple components (e.g., flight-
56 initiation distance, escape trajectory, escape speed, etc.) may vary depending on perceived

57 predation risk (Domenici & Blake, 1991, Domenici et al. 2011, Kawabata et al. 2023). Escape
58 responses of wildlife to approaching *vehicles* also appear to be dynamic and multifaceted (Lima
59 et al., 2015, Lunn et al., 2022). However, previous empirical studies (DeVault et al. 2015, Guenin
60 et al. 2024) have been limited to estimating whether a collision occurs based on only a single
61 escape response component, the distance between the animal and the vehicle the moment the
62 animal initiates escape (i.e., flight-initiation distance).

63 Recently, a mathematical framework was proposed (Lunn et al. 2026) to estimate whether
64 an animal-vehicle collision occurs by considering simultaneously multiple components of both
65 the escape response of an animal and the approaching vehicle. However, this mathematical
66 framework has yet to be applied to estimate the probability of collision with empirical data.
67 Specifically, estimates for the probability of collision have three direct applications. First,
68 estimates for the probability of collision can be used to readily translate how a given
69 management strategy might reduce economic costs (Huijser, et al., 2009, Bissonette et al., 2009,
70 Altringer, et al., 2021). Second, species-specific estimates for the probability of collision can be
71 used to improve forecasts of a species vulnerability to roadway mortality (Grilo et al., 2020,
72 Jacobson et al., 2016, Bénard et al., 2024), which is a key component in transportation
73 development infrastructure projects. Third, estimates for the probability of collision can be used
74 to identify the approach speeds for different vehicles at which a species behavioral response is
75 insufficient to prevent an impending collision and whether additional infrastructure is needed to
76 mitigate collisions.

77 Our study has two goals. First, we further develop Lunn et al.'s (2026) model to
78 generalize its applicability to estimate the probability of collision regardless of the shape of the
79 frontal surface area of the vehicle. Second, we applied this model to quantify the probability of

80 collision for the first time using parameters measured within a single empirical study and
81 analyzed how different components of a species' escape response contribute to the probability of
82 collision. More specifically, we estimated the probability of collision in a study assessing the
83 behavioral responses of Canada geese (*Branta canadensis*) to an unoccupied aerial system
84 (hereafter, UAS) approaching from different altitudes and with different light treatments (Lunn et
85 al. 2025). We selected this study because it was the only experiment for which six of the seven
86 variables needed to estimate the probability of collision with Lunn et al.'s (2026) model were
87 empirically measured (Lunn et al. 2025).

88

89 **Methods**

90 *Model overview and improvements*

91 The model proposed in *Lunn et al. (2026)*, is composed of two phases. Phase one estimates
92 whether the animal and vehicle overlap at the same location and time. Phase two estimates
93 whether the animal and the vehicle overlap in altitude, given a collision is possible. Collisions
94 occur only when the animal and vehicle share the same location at the same time (phase one) and
95 share a common altitude (phase two). Explicitly, the formulation of the model is built on several
96 assumptions (Supporting Information 1) including that the animal is within or near the trajectory
97 of the vehicle and that the trajectory of the vehicle and animal is linear and fixed after escape is
98 initiated.

99 We built upon the existing model (Lunn et al. 2026) to facilitate application to a variety
100 of different vehicles (i.e., variation in frontal surface area) and improve upon the accuracy of
101 model predictions. We made three distinct changes. First, in phase one the animal must travel
102 beyond the width of the vehicle and its own body length/width to completely clear the trajectory

103 of the vehicle, where the additional distance the animal must travel due to body length/width
104 varies depending on the escape trajectory of the animal. Herein, we include an equation to
105 estimate the additional distance the animal must travel for its body to completely clear the
106 trajectory of the vehicle based on its escape trajectory. Second, in phase one we now account for
107 the sensory motor-delay period in the estimates of the time remaining until the vehicle reaches
108 the animal, because the animal does not functionally begin to change its position within the
109 trajectory of the vehicle until after the sensory motor-delay period (Provini et al., 2012, Guenin
110 et al., 2024). Third, we adjusted phase two of the model to explicitly consider the altitude of the
111 animal to estimate whether the frontal surface of the animal and vehicle overlap as opposed to
112 inferring a probability of collision based on the frontal surface area of the vehicle alone (Lunn et
113 al. 2026).

114

115 *Phases one and two*

116 Phase one of the model in Lunn et al., 2026 estimates whether a collision is possible by
117 comparing the time the animal needs to escape the trajectory of the approaching vehicle (T_a)
118 relative to the time remaining before the vehicle reaches the animal after escape is initiated (T_v).
119 The time the animal needs to escape the trajectory of the vehicle (T_a) is calculated using equation
120 1 with the following variables: the minimum distance to safety determined by the width of the
121 vehicle (U_w), the trajectory adjusted length of the animal (l_{adj}), escape speed (S_a), escape angle
122 (θ), and sensory-motor delay as the animal reorients and begins to accelerate (δ).

123

$$T_a = \left(\frac{U_w + l_{adj}}{\frac{\sin(\theta)}{S_a}} \right) + \delta \quad (\text{Eq.1})$$

124 The total distance the animal needs to travel to clear the trajectory of the vehicle varies slightly
125 depending on the escape trajectory of the animal. Equation 2 estimates the trajectory adjusted
126 length (l_{adj}) the animal must travel to clear the trajectory of the vehicle,

$$127 \quad l_{adj} = |(G_l * \sin(\theta)) + (G_w * \cos(\theta))| \quad (\text{Eq. 2})$$

128 where the variables of G_l and G_w respectively correspond to the body length, here defined as the
129 length from beak tip to tail feathers, and width, here defined as wingspan, of the animal.

130 The time remaining until the vehicle reaches the location of the animal after the animal
131 begins to move (T_v) is calculated using equation 3 with the following variables: flight-initiation
132 distance (D_{FID}), sensory motor-delay period (δ), escape speed (S_a), and escape angle (θ) of the
133 animal, and the approach speed of the vehicle (S_v).

$$134 \quad T_v = \frac{D_{FID} - (S_v * \delta)}{S_v + (\cos(\theta) * S_a)} \quad (\text{Eq.3})$$

135 Escape speed (S_a) and trajectory (θ) of the animal affect the time the vehicle reaches the
136 location of the animal; however, only when the animal begins moving. The animal does not
137 functionally begin to change its position within the trajectory of the vehicle until after the
138 sensory motor-delay period (δ). During that period, the UAS continues to approach and as a
139 result the distance between the animal and vehicle decreases, where the decrease in distance is
140 determined by the UAS approach speed (i.e., $S_v * \delta$). If T_a (i.e., time needed to escape) is
141 greater than or equal to T_v (i.e., time remaining to successfully escape) a collision is possible,
142 where if $T_a < T_v$ a collision is entirely avoided. Phase two of the model is only applicable if
143 $T_a \geq T_v$.

144 Phase two of Lunn et al., 2026 estimates whether the animal and vehicle overlap in
145 altitude, given the location of the animal within the trajectory of the vehicle. The location of the

146 animal ($D_{collision}$) within the trajectory of the vehicle the moment the vehicle reaches the animal
 147 is calculated using equation 4 with the following variables: the animals initial location in the
 148 trajectory of the vehicle ($D_{initial}$), escape speed (S_a), escape angle (θ), and the time remaining
 149 until the vehicle reaches the location of the animal after escape initiation (T_v).

$$150 \quad D_{collision} = D_{initial} + (\cos(\theta) * S_a * (T_v)) \quad (\text{Eq. 4})$$

151 Based on the location of the animal within the trajectory of the vehicle we explicitly
 152 estimate whether the animal and vehicle overlap in altitude. To facilitate model application, we
 153 elected to estimate whether two uniform rectangular shapes overlap in a 2D plane as opposed to
 154 considering the specific shape of the vehicle. The x and y coordinates of both shapes within the
 155 2D plane correspond to the position and altitude of the vehicle and animal (Eq. 5a-5f, Fig.1).

156 Equation 5a and 5b respectively estimate the length of overlap in vehicle height and
 157 width with the animal. Equation 5a considers vehicle altitude (U_{alt}) and height (U_h) and animal
 158 altitude (G_{alt}) and height (G_h).

$$159 \quad h_{\cap} = \min\left(U_{alt} + \frac{U_h}{2}, G_{alt}\right) - \max\left(U_{alt} - \frac{U_h}{2}, G_{alt} - G_h\right) \quad (\text{Eq. 5a})$$

160 Goose altitude (G_{alt}) is defined as the part of the bird with the highest altitude (e.g., the head of
 161 the animal), where the altitude of the vehicle is defined as the midpoint point of vehicle height
 162 (U_{alt}). Equation 5b considers the width of the vehicle (U_w) and animal (G_w).

$$163 \quad w_{\cap} = \min\left(U_x + \frac{U_w}{2}, D_{collision} + \frac{U_w}{2}\right) - \max\left(U_x - \frac{U_w}{2}, -l_{adj} + (D_{collision} + \frac{U_w}{2})\right) \quad (\text{Eq. 5b})$$

164 Equation 5b assumes that the furthest and tallest edge of the animal (i.e., the head) was aligned
 165 with the center of the vehicle at the moment of escape initiation (Fig. 1, t_1). The overlap in width
 166 is determined by the trajectory adjusted length (l_{adj}) and how far the animal moved after escape
 167 initiation ($D_{collision}$), given that the animal's initial position started in alignment with the center of

168 the vehicle ($\frac{U_w}{2}$) (Fig. 1, t_2). We only considered positive values of h_ρ and w_ρ (i.e., when overlap
 169 between the vehicle and animal occurred) (Eq. 5c & 5d).

170
$$H(h_\rho) = \begin{cases} 0, & h_\rho \leq 0 \\ h_\rho, & h_\rho > 0 \end{cases} \quad (\text{Eq.5c})$$

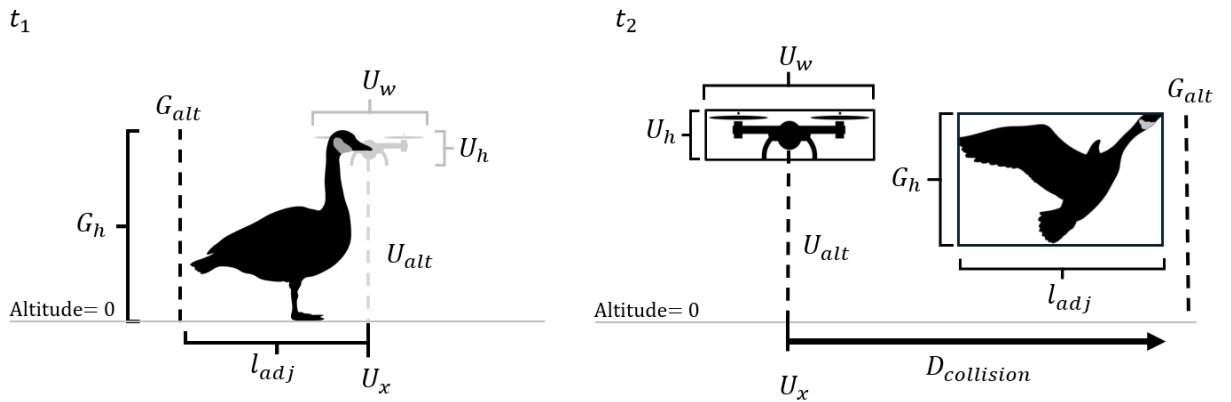
171
$$W(w_\rho) = \begin{cases} 0, & w_\rho \leq 0 \\ w_\rho, & w_\rho > 0 \end{cases} \quad (\text{Eq.5d})$$

172 Equation 5e estimates the surface area of the vehicle overlapping with the animal and then
 173 equation 5f converts that metric of overlap into a binary variable. All model estimates were made
 174 in R programing (version 4.3.2, R Core Team).

175
$$A_U = H(h_\rho) * W(w_\rho) \quad (\text{Eq. 5e})$$

176
$$P(A_u) = \begin{cases} 0, & A_u \leq 0 \\ 1, & A_u > 0 \end{cases} \quad (\text{Eq. 5f})$$

177



178
 179 Figure 1. Graphical description of the variables featured in equations 5a-5f. At t_1 prior to escape
 180 initiation it was assumed the head of the animal was aligned with the center point of the UAS
 181 and the goose was at an altitude of 0 m (i.e., a collision course). At t_2 the UAS reaches the
 182 location of the animal (i.e., the minimum bypass distance), where if a collision is possible
 183 whether the two shapes overlap is estimated.

184

185 *Model application and parameter selection*

186 We applied the model to empirical data from a behavioral experiment (Lunn et al. 2025) that
187 featured an experiment where Canada geese were approached directly with an unoccupied-aerial
188 system (hereafter, UAS) to assess how different approach types (i.e., low-altitude vs. high
189 altitude) and light treatments (i.e., light-off, light-on steady, and light-on pulsing) affected their
190 escape responses (Lunn et al. 2025). Onboard light technology tuned to the avian eye has been
191 shown to elicit early avian alert responses (Blackwell & Fernandez-Juricic et al. 2013, Blackwell
192 et al. 2012, Doppler et al. 2015), thus enabling the animal to escape earlier (i.e., longer T_v)
193 potentially reducing the probability of collision (Blackwell & Fernández-Juricic, 2013). In this
194 field study, Canada geese increased flight initiation distance and tended to move away from the
195 vehicle when the UAS approached from a higher altitude during the light-on steady & light-on
196 pulsing treatments (Lunn et al. 2025), which potentially could reduce the probability of collision.

197 For this study, we used goose flight-initiation distance (D_{FID}), escape trajectory (θ),
198 escape speed (S_a), and the sensory-motor delay (δ) for every trial measured in Lunn et al. (2025).
199 All “NA” values for flight-initiation distance (D_{FID}), escape trajectory (θ), escape speed (S_a),
200 and sensory-motor delay (δ) were assigned a value of zero. These circumstances were typically
201 due to geese hiding or ducking in response to the approaching UAS. Additionally, UAS altitude
202 (U_{alt}) at flight initiation and the mean UAS approach speed for the entire trial (S_v) were recorded
203 from the UAS flight log data (Lunn et al. 2025). UAS altitude values at flight-initiation listed as
204 “NA” due to an flight-initiation distance value of zero were imputed with the mean UAS altitude
205 values. Further, UAS altitude values at flight initiation that exceeded the maximum height of the
206 arena (1.82 m) were subsequently limited to a value of 1.82 m.

207 The small quadcopter UAS used in Lunn et al. 2025 was a DJI Mavic 3 classic.
208 Specifically, the dimensions were 0.347 m in length x 0.527 m in width x 0.107 m in height

209 (<https://www.dji.com/mavic-3-classic/specs>, Dia-Jiang Innovations, Shenzhen, China), where the
210 vehicle width also included the additional width attributable to propeller length
211 (<https://store.dji.com/product/dji-mavic-3-low-noise-propellers>, Dia-Jiang Innovations,
212 Shenzhen, China). The dimensions of the light onboard the UAS (Lume Cube RGB Panel Pro
213 2.0, <https://lumecube.com/products/panel-pro> , Toledo, OH, U.S.A) were 0.152 m in width and
214 0.08 m in height. The height used in equations 5a-5f was a combination of both the UAS and the
215 light (i.e., 0.27 m, the height of two lights stacked and the UAS), but the width of the light did
216 not extend beyond the UAS. For the Canada goose dimensions, we selected a single value for the
217 length and width based on empirical data of goose anatomical measurements: 1.025 m length
218 (Bellrose, 1976, Mowbray et al. 2020), 1.485 m width (Hanson, 1951, Sibley, 2014) (i.e., the
219 wingspan), 0.513 m in height (i.e., half the length).

220 Lunn et al. 2025 did not measure the altitude of the goose during the escape phase.
221 Consequently, to estimate $P(A_u)$ in phase two of the model, we simulated goose altitude (G_{alt})
222 values. For each empirical trial, we simulated 1,000,000 altitude values from a uniform
223 distribution ranging from 0.256 to 1.82 m. A minimum value of 0.256 m was selected because it
224 was half the height of the goose (i.e., attempting to crouch) and a maximum value of 1.82 was
225 selected because of the maximum height of the experimental arena (1.82 m) (i.e., attempting to
226 take flight). We estimated the probability of altitudinal overlap for each trial as the total number
227 of altitudes wherein the animal overlapped with the vehicle divided by the number of simulated
228 altitude values (i.e., 1,000,000).

229 We estimated whether the vehicle and the animal did or did not share a common altitude
230 (i.e., a binary variable) based on a threshold value (see below) for the probability of altitudinal
231 overlap, where values greater than or equal to threshold were labelled as overlapping in altitude

232 while values less than threshold were considered to not overlap in altitude. We selected a
233 threshold value for the probability of altitudinal overlap based on a value of 28% based on the
234 results of a sensitivity analysis examining how different threshold values from 0% to 100%
235 affected the estimated total number of trials with altitudinal overlap (Supporting Information 2).
236 No trial had a probability of altitudinal overlap greater than or equal to 68% but 131 trials had a
237 probability of altitudinal overlap for a threshold greater than 0%. Consequently, we selected the
238 median value of 34% (i.e., 118 trials) as the threshold for the probability of altitudinal overlap as
239 a compromise between high sensitivity (i.e., a threshold of greater than 0%) and higher
240 specificity at the cost of lower sensitivity (i.e., a threshold of greater than 68%).

241

242 *Experimental treatments and the probability of collision*

243 We demonstrated the utility of the model by assessing how the experimental treatments from
244 Lunn et al. (2025) affected the model estimates of the probability of collision. We used a
245 generalized linear model with the same statistical model structure in the analysis of the
246 probability of collision estimates as Lunn et al. (2025), so the assessments of approach type and
247 light treatment were comparable to the assessments for each element of the behavioral response
248 measured. Specifically, each model included three categorical variables (light treatment,
249 approach type treatment, approach speed (i.e., slow: 0.27 m/s to 5.52 m/s, vs. fast: 5.52 m/s to
250 8.09 m/s), three continuous variables (wind speed, goose weight, irradiance) and three different
251 interaction effects (light treatment and approach type treatment, light treatment and approach
252 speed, and approach type treatment and approach speed).

253 We used the *stats* package to run our generalized linear model (R Core Team). We
254 determined significance for each independent variable with type 3 sum of squares analysis from

255 the *car* package (Fox et al., 2012). For each treatment condition and the corresponding
256 interaction between treatments we present the model estimated means with the *emmeans* package
257 (Lenth et al., 2019). Additionally, we used the *binom* package to estimate the confidence
258 intervals using the Agresti-Coull method (Aho & Bowyer, 2014, Dorai-Raj, 2022). Whenever a
259 treatment with more than two levels was significant, we utilized the tukey method to test for
260 significance among the different levels via the *emmeans* package (Lenth, 2017).

261

262 *Effect sizes of model parameters*

263 The mathematical model included several parameters (see section *Model application and*
264 *parameter selection*) to estimate the probability of collision. We investigated the relative
265 contribution of each parameter on the estimated probability of collision using a generalized
266 linear model that considered all model inputs as independent variables using the *stats* R package
267 (R Core Team). Specifically, the statistical model included goose flight-initiation distance,
268 escape speed, escape trajectory, sensory-motor delay period, UAS altitude, and UAS speed. We
269 estimated the model predicted effect size using the *emmeans* package (Lenth, 2017). Herein we
270 estimated both Tjur's R^2 for the entire model (Tjur, 2009) and the partial omega-squared for each
271 independent variable (i.e., ω_p^2) with the *effectsize* package (Ben-Shachar et al., 2020). We
272 categorized ω_p^2 as either being either a “very small”, “small”, “medium”, or “large” effect based
273 on Cohen 1992.

274 We conducted all statistical analyses and developed all figures in R version 4.3.2 (R Core
275 Team, 2024). All code, datasets and metadata necessary to reproduce this study are available at
276 OSF [https://osf.io/9rh47/overview?view_only=1750d6840d3a4478bec0432b2fec2424].

277 Throughout the results, we present the model estimated means and 95% confidence intervals
278 within brackets.

279

280

281 **Results**

282

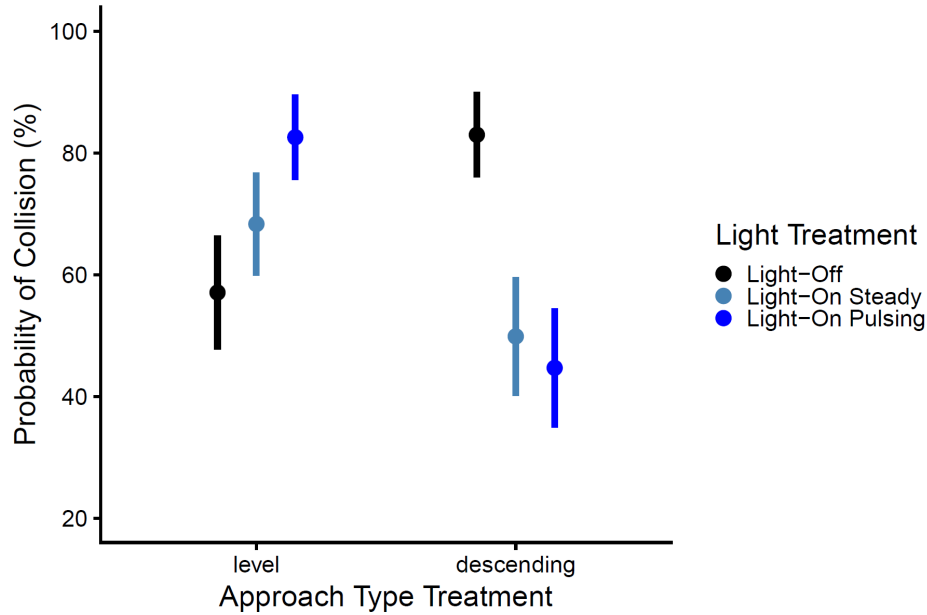
283 *Experimental treatments and the probability of collision*

284 The probability of collision for the light-on steady treatment (59.44%, [48.10%, 71.95%]) and
285 light-on pulsing treatment (66.20, [49.92%, 73.94%]) was respectively, 12.38% and 5.62% lower
286 relative to the light-off treatment (71.82, [57.58%, 79.82%]), with light treatment significantly
287 affecting the probability of collision (Table 1), but no significant differences between different
288 light treatment levels. The probability of collision for the descending approach treatment
289 (61.21%, [50.28%, 70.19%]) was 9.28% lower compared to the level approach treatment (70.49,
290 [58.09%, 76.66%]), without a significant effect of approach treatment (Table 1). However, light
291 treatment and approach treatment interacted significantly (Table 1, Figure 1). More specifically,
292 for level approach treatments, the probability of collision for both the light-on steady (68.34%,
293 [50.03%, 81.54%]) and light-on pulsing (82.59%, [60.96%, 89.27%]) treatments increased by
294 9.92% and 25.47% respectively relative to the light-off treatment (57.09%, [40.74%,73.61%]).
295 However, for descending approach treatments, the probability of collision for both the light-on
296 steady (49.88%, [36.14%, 69.77%]) and light-on pulsing (44.71%, [27.57%, 62.70%]) treatments
297 decreased by 34.38% and 37.24%, respectively, relative to the light-off treatment (83.00%,
298 [64.32%, 91.48%]). Within the interaction both the light-on steady ($z = 2.487, p = 0.035$) and
299 light-on pulsing treatments ($z = 2.844, p = 0.012$) were significantly different than the light-off
300 treatment but only during descending approaches.

301
302
303
304
305
306
307
308
309

Table 1. Generalized linear model results for probability of collision and independent variables and covariates used in the analysis of Lunn et al., 2025.

<i>Generalized Linear Model</i>	X^2	<i>d.f</i>	<i>P</i>
Probability of Collision:			
<i>Altitudinal Overlap Threshold > 34%</i>			
<i>Light treatment</i>	7.300	2	0.026*
<i>Approach type treatment</i>	0.939	1	0.333
<i>Goose Weight</i>	2.536	1	0.111
<i>Speed</i>	0.794	1	0.373
<i>Irradiance</i>	0.004	1	0.952
<i>Wind Speed</i>	0.071	1	0.790
<i>Light Treatment X Approach type treatment</i>	12.202	2	0.002**
<i>Light Treatment: X Speed</i>	0.689	2	0.708
<i>Approach type treatment X Speed</i>	3.696	1	0.055



310

311 Figure 2. The estimated marginal means and S.E for the significant interaction effect between
 312 light and approach type treatment reported from the generalized linear model for the probability
 313 of collision estimates

314

315 *Effect sizes of model parameters*

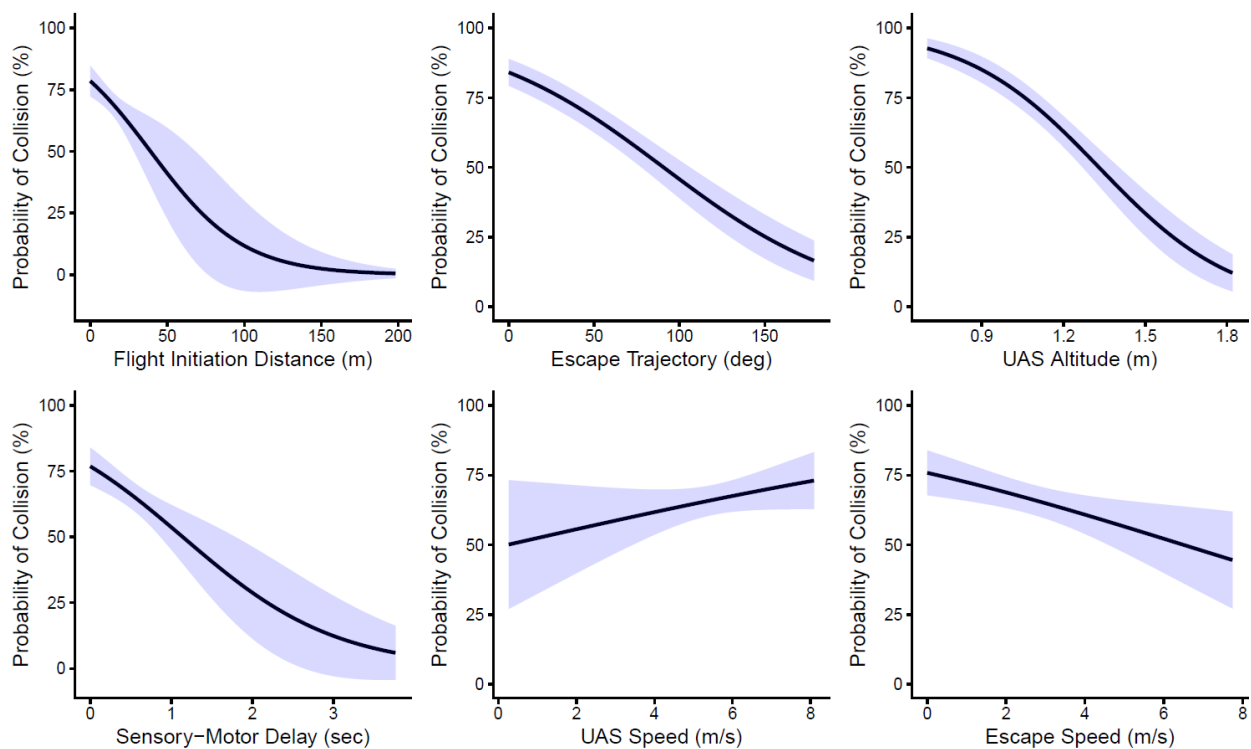
316 After including the mathematical model inputs in a generalized linear model on the probability of
 317 collision, the variable with the largest effect size was flight-initiation distance (ω_p^2 of 0.26, large
 318 effect), where a change in flight-initiation distance from 0 to 198.17 m resulted in a decrease in
 319 the probability of collision from 78.54% to 0.51% with an inflection point of 38.84 m (Fig.3a).

320 The variable with the second largest effect size was escape trajectory (ω_p^2 of 0.20, medium
 321 effect), where a change in escape trajectory from 0 to 178.84° resulted in a decrease in the
 322 probability of collision from 84.10% to 16.57% with an inflection point of 90.33 deg (Fig.3b).

323 The variable with the third largest effect size was UAS altitude (ω_p^2 of 0.14, medium effect),
 324 where a change in UAS altitude from 0.7 to 1.82 m resulted in a decrease in the probability of
 325 collision from 92.74% to 12.15% with an inflection point of 1.32 m (Fig.3c). The variable with

326 the fourth largest effect size was sensory-motor delay (ω_p^2 of 0.03, small effect), where a change
 327 in a sensory-motor delay from 0 to 3.77 seconds resulted in a decrease in the probability of
 328 collision from 76.87% to 5.94%, with an inflection point of 1.14 seconds (Fig.3d). The variable
 329 with the fifth largest effect size was UAS approach speed (ω_p^2 of <0.01, very small effect), where
 330 a change in UAS approach speed from 0.27 to 8.09 m/s resulted in an increase in the probability
 331 of collision from 50.12% to 73.05% with no inflection point (Fig.3e). Lastly, the variable with
 332 the smallest effect size was escape speed (ω_p^2 of <0.01, very small effect), where a change in
 333 escape speed from 0 to 7.74 m/s resulted in a decrease in the probability of collision from
 334 75.84% to 44.56% with an inflection point of 6.48 m/s (Fig.3f). The overall model had a Tjur's
 335 R^2 value = 0.497, which is deemed as a large effect size.

336



337

338 Figure 3. The black curve is the predicted probability of collision from the generalized linear
 339 model for a given value of each mathematical model input based on empirical data from Lunn et

340 al. (2025). The blue shading represents the standard error estimates form the generalized linear
341 model.

342

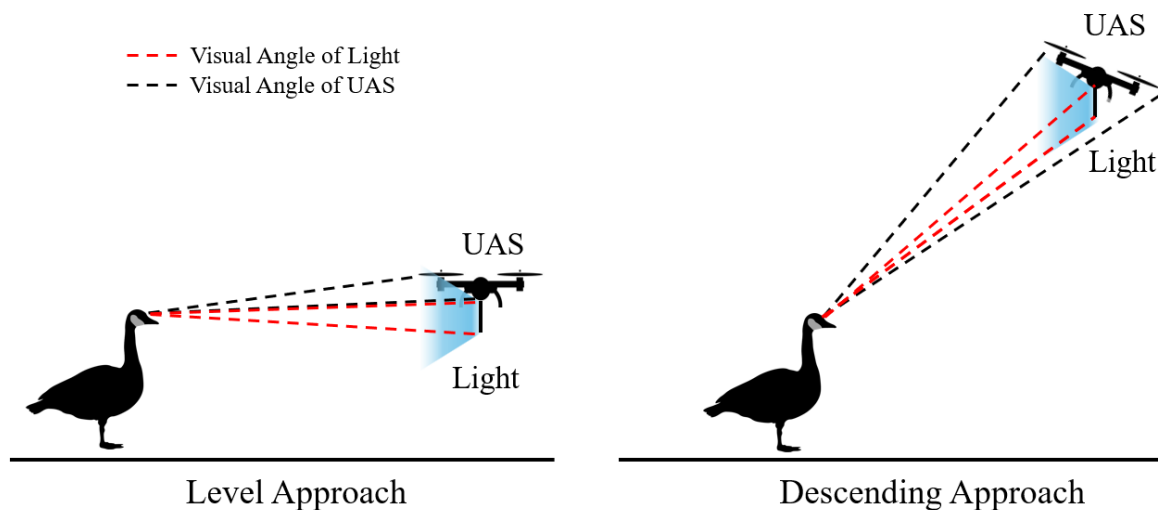
343

344 **Discussion**

345 We propose a more generalized version of an existing mathematical model to estimate the
346 probability of collision between a bird and an approaching vehicle. We applied this model to
347 estimate the probability of collision for an empirical experiment where a UAS approached a
348 Canada goose testing the effects of different onboard-lights and approach types. Overall, the
349 effect of light tuned to the visual system of Canada geese on the probability of collision heavily
350 depended on how the UAS approached the animal. Generally, for level UAS approach treatments
351 the light-on treatments tended to increase the probability of collision by 12 to 25 percentage
352 points, but for the descending approach treatments the light-on treatments tended to decrease the
353 probability of collision by 27 to 30 percentage points. The variable with the largest effect on
354 determining whether an estimated collision occurred was flight-initiation distance, followed by
355 UAS altitude, and escape trajectory.

356 One possible explanation for the increase in the probability of collision during level flight
357 approaches and, alternatively, a decrease in the probability of collision for descending
358 approaches is that the light masked the presence of the UAS for level flights but facilitated
359 detection of the UAS for descending flights. Animals have limited attention that is selectively
360 allocated (Dukas & Kamil, 2000, & Blumstein et al., 2010). For onboard lighting to be effective
361 it should draw the animal's attention towards the approaching vehicle, but not mask the presence
362 of the vehicle, such that an animal can distinguish the vehicle from the light because mortality
363 risk stems from vehicle size and speed (Bernhardt et al., 2010, DeVault et al., 2015). Differences

364 in the ratio of UAS to LED light surface area may have resulted in the light masking the
365 approaching vehicle during level approaches but drawing the animal's attention towards the
366 vehicle during descending approaches. For level approaches, we estimated that the ratio of UAS
367 to LED light surface area was 1.39 to 1 based on the frontal surface of the UAS (Fig. 4);
368 however, for descending approaches, the ratio was 4.51 to 1, potentially allowing greater visual
369 access to the bottom of the UAS and making it relatively easier to differentiate the UAS from the
370 LED light (Fig. 4). This masking phenomenon might explain why during low ambient light
371 conditions we observe that light stimuli hinder the escape response of some species (Erritzoe et
372 al., 2003, Guenin et al., 2024) because the increased sensitivity to light in the visual system in
373 low light conditions (Lind et al., 2014) might prevent the animal from detecting the vehicle
374 (Blackwell et al., 2014, DeVault et al., 2020). Consequently, lights aimed at mitigating animal-
375 vehicle collisions should maintain a higher ratio of vehicle to LED light surface area.
376 Practically, this could be achieved by using narrower beam angles (i.e., reducing the dispersion
377 of light) to reduce the probability of masking the vehicle.

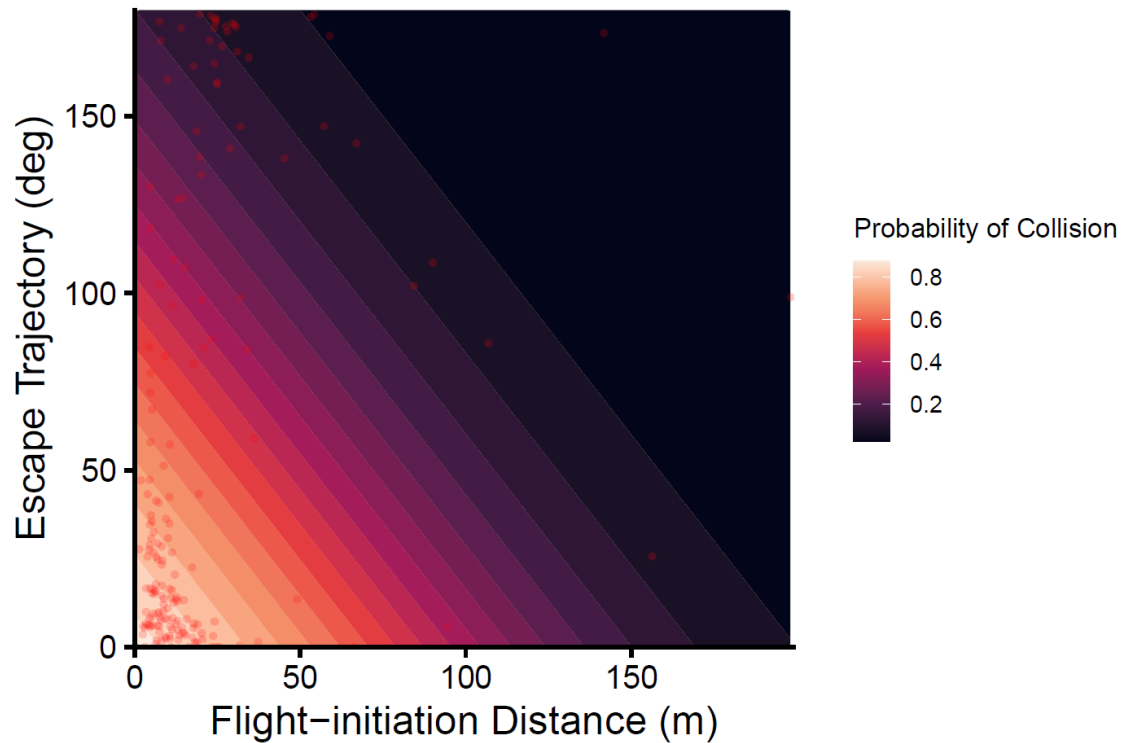


379 Figure 4. Visual illustration of the difference in surface area ratio geese had visual access to
380 between the two different approach type treatments. Red lines indicate the visual angle of the
381 light where black lines indicate the visual angle of the UAS.

382

383 Studies of animal vehicle collisions have focused overwhelmingly on differences in
384 flight-initiation distance, where longer flight-initiation distances have been assumed to translate
385 to a lower probability of collision (DeVault et al., 2015, Blackwell et al., 2019). However, escape
386 responses are a dynamic and interdependent sequence of behaviors (Lima & Dill, 1990, Cooper
387 & Blumstein, 2015, Evans et al., 2019, Branco & Redgrave, 2020). While flight-initiation
388 distance has a large effect on the probability of collision (Lunn et al. 2026), and herein was the
389 variable with the largest effect size, our results suggest that the assumption that a long enough
390 flight-initiation distances will completely reduce the probability of collision is incorrect because
391 the effectiveness of flight-initiation distance simultaneously depends on other components of an
392 escape response. Figure 5 illustrates how escape trajectory, another component of an escape
393 response, modulates the effect of flight-initiation distance on the probability of collision for
394 different treatment combinations, where the probability of collision is based on the estimates
395 from the generalized linear model built with model inputs. If the probability of collision was
396 completely dependent on flight-initiation distance the contour lines, which represent a 5%
397 change in the probability of collision, would be completely vertical. However, the contour lines
398 have a decreasing slope indicating that the probability of collision is regulated by both flight
399 initiation distance and escape trajectory. Figure 5 shows that even the longest flight-initiation
400 distance observed (i.e., 198 m) had a probability of collision $> 0\%$ for an escape trajectory
401 directly towards the UAS. This finding suggests that a threshold flight-initiation distance long
402 enough to make all other components of the escape response irrelevant either does not exist or is
403 extremely rare. The empirically observed values of flight-initiation distance and escape trajectory
404 suggests that Canada geese, while at times did change flight-initiation distance to reduce the

405 probability of collision, more readily adjusted escape trajectory to manage the perceived
406 mortality risk especially for shorter flight-initiation distances.



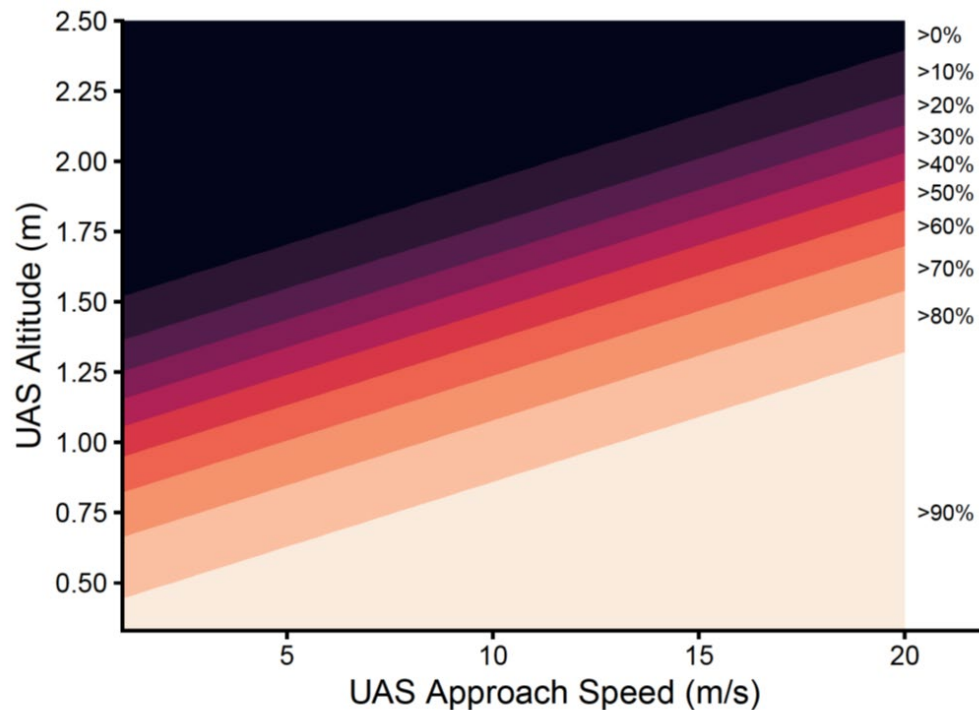
407
408 Figure 5. Flight-initiation distance plotted against escape trajectory where the shading represents
409 differences in the predicted probability of collision from the generalized linear built with model
410 inputs. Different shades represent bins of 5% probability of collision. Red dots are the empirical
411 values observed in Lunn et al., 2025 for flight-initiation distance and escape trajectory.
412

413 In the predator-prey literature, a common assumption is that a flight-initiation distance of
414 zero is associated with prey mortality because predators actively target prey (Ydenberg & Dill,
415 1986, Broom & Ruxton,2005). However, in the context of animal-vehicle collisions, our findings
416 challenge this assumption. The intercept of our generalized linear model estimated the
417 probability of collision for a flight-initiation distance of zero to actually be 69.41%, providing
418 evidence that a flight-initiation distance of zero can result in successful collision avoidance with
419 a vehicle. This is likely due to the interplay between vehicle size and shape, animal size and
420 shape, and whether the vehicle approaches directly or indirectly (i.e., the animal is near but

421 outside of the trajectory of the vehicle). For example, a bird within the path trajectory of an
422 aircraft can pass underneath its wing and still avoid a collision (Lunn et al., 2026). Consequently,
423 a flight-initiation distance of zero in some bird species might be a feature of their vehicle
424 collision avoidance behavior and might in part explain why in previous studies birds did not flee
425 when approached by a vehicle (Blackwell et al. 2019, Guenin et al. 2024) or fled only after the
426 vehicle has passed (Pfeiffer et al. 2025).

427 UAS have been proposed as a potential solution to haze birds from areas of
428 anthropogenic activity, such as landfills, airports, and buildings (Pfeiffer et al., 2021, Pfeiffer et
429 al., 2023, White et al., 2025). Generally, the literature suggests that lower altitude flights directly
430 targeting individuals tend to be more effective at dispersing birds (Vas et al., 2015, Egan et al.,
431 2020, Pfeiffer et al., 2025). However, low altitude flights, especially near wildlife can result in a
432 collision damaging both the bird and UAS (Lunn et al., 2025), which can negatively affect
433 animal welfare. We applied the model to a hazing scenario to demonstrate its utility at providing
434 general recommendations about how UAS flight altitude and speed might be safely flown to
435 minimize the probability of harming birds while hazing. Using the generalized linear model built
436 with the model inputs, we predicted the probability of collision as UAS approach speed
437 increased from 1 to 20 m/s and UAS altitude increased from 0.5 to 2.6 m for every trial,
438 assuming all other components of the escape response of the animal remained the same.
439 Generally, an altitude of 2.4 m or higher regardless of UAS speed had a 0% probability of
440 colliding with Canada geese (Fig. 6). Alternatively, the absolute minimum altitude a UAS can
441 still maintain a 0% probability of collision is 1.51 m at the slowest possible approach speed (i.e.,
442 1 m/s) (Fig. 6). Based on the slope of the contour line (i.e., the threshold between a 0 and 5%
443 probability of collision), the model suggests that UAS operators hazing Canada geese should

444 increase altitude by 4.6 cm for every 1 m/s increase in UAS approach speed to maintain a 0%
445 probability of collision (Fig. 6).



446
447 Figure 6. The relationship between UAS approach speed (x-axis), altitude (y-axis) and the
448 predicted probability of collision (color shading) based on the generalized linear model built with
449 model inputs. Each contour line denotes the separation of the probability of collision in 10%
450 bins.
451

452 We presented the first application to empirical data of a mathematical framework directly
453 connecting multiple components of an animal escape response to estimate the probability of
454 collision with an approaching vehicle. The results of our approach yield two key insights that can
455 be incorporated into future research on animal-vehicle collisions: (1) while longer flight-
456 initiation generally decrease the probability of collision, importantly they also depend on other
457 components of the animals escape response; and (2) a flight-initiation distance of zero does not
458 necessarily result in a collision occurring. Further, the model provides a step forward in
459 improving the accuracy of transportations infrastructures mortality effect on wildlife. Animal-

460 vehicle collision and wildlife-road mortality research is often severely limited by “survivor” bias,
461 where often we only observe the consequences of collisions, assuming a wildlife-vehicle
462 interaction occurred. Yet there is limited to no understanding of 1) how many total wildlife-
463 vehicle interactions occurred, 2) how many collisions occurred but were not detected, and 3) how
464 many of those interactions did not result in a collision. Failing to account for any of these
465 unknowns could consequently result in either over or underestimates of the mortality impact of
466 transportation infrastructure on wildlife and subsequently result in misguided and ineffective
467 management strategies. Our model can quantitatively provide answers to how many interactions
468 did not result in a collision by pairing the estimated probability of collision based on the escape
469 response of the animal with the frequency of collisions observed (i.e., carcasses/reported
470 collisions) to provide more accurate estimates for the mortality risk caused by transportation
471 infrastructure.

472

473 **References**

474 Ascensão, F., Clevenger, A., Santos-Reis, M., Urbano, P. and Jackson, N., 2013. Wildlife–vehicle
475 collision mitigation: Is partial fencing the answer? An agent-based model approach. *Ecological*
476 *Modelling*, 257, pp.36-43. <https://doi.org/10.1016/j.ecolmodel.2013.02.026>

477 Aho, K. and Bowyer, R.T., 2015. Confidence intervals for ratios of proportions: implications for
478 selection ratios. *Methods in Ecology and Evolution*, 6(2), pp.121-132.
479 <https://doi.org/10.1111/2041-210X.12304>

480 Altringer, L., Navin, J., Begier, M.J., Shwiff, S.A. and Anderson, A., 2021. Estimating wildlife
481 strike costs at US airports: A machine learning approach. *Transportation Research Part D:*
482 *Transport and Environment*, 97, p.102907. <https://doi.org/10.1016/j.trd.2021.102907>

483

484 Ben-Shachar, M.S., Makowski, D., Lüdecke, D., Patil, I., Wiernik, B.M., Kelley, K., Stanley, D.,
485 Burnett, J. and Karreth, J., 2021. Package ‘effectsize’. *R Package*.

486

487 Bernhardt, G.E., Blackwell, B.F., DeVault, T.L. and Kutschbach-Brohl L., 2010. Fatal injuries to
488 birds from collisions with aircraft reveal anti-predator behaviours. *Ibis*, 152(4), pp.830-834.
489 <https://doi.org/10.1111/j.1474-919X.2010.01043.x>

490

491 Blackwell, B. F., & Bernhardt, G. E. (2004). Efficacy of aircraft landing lights in stimulating
492 avoidance behavior in birds. *The Journal of wildlife management*, 68(3), 725-732.
493 <https://doi.org/10.2193/2008-014>
494

495 Blackwell, B.F., DeVault, T.L., Seamans, T.W., Lima, S.L., Baumhardt, P. and Fernández-Juricic,
496 E., 2012. Exploiting avian vision with aircraft lighting to reduce bird strikes. *Journal of Applied*
497 *Ecology*, 49(4), pp.758-766. <https://doi.org/10.1111/j.1365-2664.2012.02165.x>
498

499 Blackwell, B.F., Fernández-Juricic, E., 2013. Behavior and Physiology in the Development
500 and. *Wildlife in airport environments: preventing animal–aircraft collisions through science-*
501 *based management*, p.11–22, 1st edn. Baltimore, MD: Johns Hopkins University Press
502

503 Blackwell, B.F. and Seamans, T.W., 2009. Enhancing the perceived threat of vehicle approach to
504 deer. *The Journal of Wildlife Management*, 73(1), pp.128-135.
505

506 Blackwell, B.F., Seamans, T.W., DeVault, T.L., Lima, S.L., Pfeiffer, M.B. and Fernández-Juricic,
507 E., 2019. Social information affects Canada goose alert and escape responses to vehicle
508 approach: implications for animal–vehicle collisions. *PeerJ*, 7, p.e8164..
509 <https://doi.org/10.7717/peerj.8164>.
510

511 Belant, J. L. (2011). *Bird harassment, repellent, and deterrent techniques for use on and near*
512 *airports* (Vol. 23). Transportation Research Board.

513 Bellrose, F.C., 1976. *Ducks, geese and swans of North America* (pp. 541-pp).

514 Bénard, A., Lengagne, T. and Bonenfant, C., 2024. Integration of animal movement into wildlife-
515 vehicle collision models. *Ecological Modelling*, 492, p.110690.
516 <https://doi.org/10.1016/j.ecolmodel.2024.110690>

517 Bissonette, J.A., Kassar, C.A. and Cook, L.J., 2008. Assessment of costs associated with deer–
518 vehicle collisions: human death and injury, vehicle damage, and deer loss. *Human-Wildlife*
519 *Conflicts*, 2(1), pp.17-27. <https://www.jstor.org/stable/24875102>

520 Blumstein, D.T., 2010. Flush early and avoid the rush: a general rule of antipredator
521 behavior?. *Behavioral Ecology*, 21(3), pp.440-442. <https://doi.org/10.1093/beheco/arq030>

522 Branco, T. and Redgrave, P., 2020. The neural basis of escape behavior in vertebrates. *Annual*
523 *review of neuroscience*, 43(1), pp.417-439. <https://doi.org/10.1146/annurev-neuro-100219-122527>
524

525 Brieger, F., Kämmerle, J.L., Hagen, R. and Suchant, R., 2022. Behavioural reactions to
526 oncoming vehicles as a crucial aspect of wildlife-vehicle collision risk in three common wildlife
527 species. *Accident Analysis & Prevention*, 168, p.106564.
528 <https://doi.org/10.1016/j.aap.2021.106564>

529 Broom, M. and Ruxton, G.D., 2005. You can run—or you can hide: optimal strategies for cryptic
530 prey against pursuit predators. *Behavioral Ecology*, 16(3), pp.534-540.
531 <https://doi.org/10.1093/beheco/ari024>

- 532 Cohen, J., 1992. Statistical power analysis. *Current directions in psychological science*, 1(3),
533 pp.98-101. <https://doi.org/10.1111/1467-8721.ep10768783>
- 534 Conover, M.R., 2019. Numbers of human fatalities, injuries, and illnesses in the United States
535 due to wildlife. *Human-Wildlife Interactions*, 13(2), pp.264-276.
536 <https://www.jstor.org/stable/27316125>
- 537 Cooper, W.E. and Blumstein, D.T. eds., 2015. *Escaping from predators: an integrative view of*
538 *escape decisions*. Cambridge University Press.
- 539 Domenici, P., Blagburn, J.M. and Bacon, J.P., 2011. Animal escapology I: theoretical issues and
540 emerging trends in escape trajectories. *Journal of Experimental Biology*, 214(15), pp.2463-2473.
541 <https://doi.org/10.1242/jeb.029652>.
- 542 Domenici, P. and Blake, R.W., 1991. The kinematics and performance of the escape response in
543 the angelfish (*Pterophyllum eimekei*). *Journal of Experimental Biology*, 156(1), pp.187-205.
544 <https://doi.org/10.1242/jeb.156.1.187>
- 545 Doppler, M.S., Blackwell, B.F., DeVault, T.L. and Fernández-Juricic, E., 2015. Cowbird
546 responses to aircraft with lights tuned to their eyes: Implications for bird–aircraft collisions. *The*
547 *Condor: Ornithological Applications*, 117(2), pp.165-177. [https://doi.org/10.1650/CONDOR-14-](https://doi.org/10.1650/CONDOR-14-157.1)
548 [157.1](https://doi.org/10.1650/CONDOR-14-157.1)
- 549 DeVault, T.L., Blackwell, B.F. and Belant, J.L. eds., 2013. *Wildlife in airport environments:*
550 *preventing animal–aircraft collisions through science-based management*. JHU Press.
- 551 DeVault, T.L., Blackwell, B.F., Seamans, T.W., Lima, S.L. and Fernández-Juricic, E., 2015.
552 Speed kills: ineffective avian escape responses to oncoming vehicles. *Proceedings of the Royal*
553 *Society B: Biological Sciences*, 282(1801). <https://doi.org/10.1098/rspb.2014.2188>.
- 554 DeVault, T. L., Seamans, T. W., & Blackwell, B. F. (2020). Frontal vehicle illumination via rear-
555 facing lighting reduces potential for collisions with white-tailed deer. *Ecosphere*, 11(7), e03187.
556 <https://doi.org/10.1002/ecs2.3187>
- 557 Dorai-Raj S., 2022. Package ‘binom’: Binomial Confidence Intervals for Several
558 Parameterizations. *R package version* 1(1.1).
- 559 Dukas, R. and Kamil, A.C., 2000. The cost of limited attention in blue jays. *Behavioral*
560 *Ecology*, 11(5), pp.502-506. <https://doi.org/10.1093/beheco/11.5.502>
- 561 Egan, C.C., Blackwell, B.F., Fernández-Juricic, E. and Klug, P.E., 2020. Testing a key
562 assumption of using drones as frightening devices: Do birds perceive drones as risky?. *The*
563 *Condor*, 122(3), p.duaa014. <https://doi.org/10.1093/condor/duaa014>
- 564 Erritzoe, J., Mazgajski, T.D. and Rejt, Ł., 2003. Bird casualties on European roads—a
565 review. *Acta Ornithologica*, 38(2), pp.77-93. <https://doi.org/10.3161/068.038.0204>
- 566 Evans, D.A., Stempel, A.V., Vale, R. and Branco, T., 2019. Cognitive control of escape
567 behaviour. *Trends in cognitive sciences*, 23(4), pp.334-348.
568 <https://doi.org/10.1016/j.tics.2019.01.012>

569 Fox, J., Weisberg, S., Adler, D., Bates, D., Baud-Bovy, G., Ellison, S., Firth, D., Friendly, M.,
570 Gorjanc, G., Graves, S. and Heiberger, R., 2012. Package ‘car’. Vienna: R Foundation for
571 Statistical Computing, 16(332), p.333.

572 Hanson, H.C., 1951. A morphometrical study of the Canada goose, *Branta canadensis* interior
573 Todd. *The Auk*, 68(2), pp.164-173.

574 Harris, R.E. and Davis, R.A., 1998. Evaluation of the efficacy of products and techniques for
575 airport bird control. *LGL Limited for Aerodrome Safety Branch, Transport Canada*, 1, pp.425-31.

576 Huijser, M.P., Fairbank, E.R., Camel-Means, W., Graham, J., Watson, V., Basting, P. and Becker,
577 D., 2016. Effectiveness of short sections of wildlife fencing and crossing structures along
578 highways in reducing wildlife–vehicle collisions and providing safe crossing opportunities for
579 large mammals. *Biological conservation*, 197, pp.61-68.
580 <https://doi.org/10.1016/j.biocon.2016.02.002>

581 Huijser, M. P., Duffield, J. W., Clevenger, A. P., Ament, R. J., & McGowen, P. T. (2009). Cost–
582 benefit analyses of mitigation measures aimed at reducing collisions with large ungulates in the
583 United States and Canada: a decision support tool. *Ecology and society*, 14(2).
584 <https://www.jstor.org/stable/26268301>

585 Huijser, M.P., McGowan, P., Fuller, J., Hardy, A., Kociolek, A.V., Clevenger, A. P., Smith, D.,
586 Ament, R., 2008. Wildlife-vehicle collision reduction study: report to congress. No. FHWA-
587 HRT-08-034. <https://rosap.nrl.bts.gov/view/dot/88021>

588 Glista, D.J., DeVault, T.L. and DeWoody, J.A., 2009. A review of mitigation measures for
589 reducing wildlife mortality on roadways. *Landscape and urban planning*, 91(1), pp.1-7.
590 <https://doi.org/10.1016/j.landurbplan.2008.11.001>

591 Grilo, C., Borda-de-Água, L., Beja, P., Goolsby, E., Soanes, K., le Roux, A., Koroleva, E.,
592 Ferreira, F.Z., Gagné, S.A., Wang, Y. and González-Suárez, M., 2021. Conservation threats from
593 roadkill in the global road network. *Global Ecology and Biogeography*, 30(11), pp.2200-2210.
594 <https://doi.org/10.1111/geb.13375>

595 Grilo, C., Koroleva, E., Andrášik, R., Bíl, M. and González-Suárez, M., 2020. Roadkill risk and
596 population vulnerability in European birds and mammals. *Frontiers in Ecology and the*
597 *Environment*, 18(6), pp.323-328. <https://doi.org/10.1002/fee.2216>

598 Guenin, S., Pakula, C.J., Skaggs, J., Fernández-Juricic, E. and DeVault, T.L., 2024. Inefficacy of
599 mallard flight responses to approaching vehicles. *PeerJ*, 12, p.e18124.
600 <https://doi.org/10.7717/peerj.18124>

601 Lenth, R., Singmann, H., Love, J., Buerkner, P. and Herve, M., 2019. Package ‘emmeans’. *R*
602 *package version*, 1(3.2).

603 Lima, S.L. and Dill, L.M., 1990. Behavioral decisions made under the risk of predation: a review
604 and prospectus. *Canadian journal of zoology*, 68(4), pp.619-640. <https://doi.org/10.1139/z90-092>

605 Lima, S.L., Blackwell, B.F., DeVault, T.L. and Fernández-Juricic, E., 2015. Animal reactions to
606 oncoming vehicles: a conceptual review. *Biological Reviews*, 90(1), pp.60-76.
607 <https://doi.org/10.1111/brv.12093>

608 Loss, S.R., Will, T. and Marra, P.P., 2015. Direct mortality of birds from anthropogenic
609 causes. *Annual Review of Ecology, Evolution, and Systematics*, 46(1), pp.99-120.
610 <https://doi.org/10.1146/annurev-ecolsys-112414-054133>

611 Lunn, R.B., Blackwell, B., Baumhardt, P., Talbot, A., Di Domenico, I. and Fernández-Juricic, E.,
612 2025. Light tuned to the avian eye elicits early detection and escape from an approaching
613 aircraft. *Royal Society Open Science*, 12(6). <https://doi.org/10.1098/rsos.250047>

614 Lunn, R.B., Blackwell, B.F., DeVault, T.L. and Fernández-Juricic, E., 2022. Can we use
615 antipredator behavior theory to predict wildlife responses to high-speed vehicles?. *PLoS*
616 *One*, 17(5), p.e0267774. <https://doi.org/10.1371/journal.pone.0267774>

617 Lunn, R.B., Blackwell, B.F. and Fernández-Juricic, E., 2026. A model to quantify the probability
618 of collision between birds and aircraft: Applications for onboard lighting. *Ecological*
619 *Applications*, 36(3), p.e70227. <https://doi.org/10.1002/eap.70227>

620 Mammeri, A., Zhou, D. and Boukerche, A., 2016. Animal-vehicle collision mitigation system for
621 automated vehicles. *IEEE Transactions on Systems, Man, and Cybernetics: Systems*, 46(9),
622 pp.1287-1299. doi: 10.1109/TSMC.2015.2497235

623

624 Moore, L.J., Petrovan, S.O., Bates, A.J., Hicks, H.L., Baker, P.J., Perkins, S.E. and Yarnell, R.W.,
625 2023. Demographic effects of road mortality on mammalian populations: a systematic
626 review. *Biological Reviews*, 98(4), pp.1033-1050. <https://doi.org/10.1111/brv.12942>

627 Mowbray, T. B., C. R. Ely, J. S. Sedinger, and R. E. Trost (2020). Canada Goose (*Branta*
628 *canadensis*), version 1.0. In Birds of the World (P. G. Rodewald, Editor). Cornell Lab of
629 Ornithology, Ithaca, NY, USA. <https://doi.org/10.2173/bow.cangoo.01>

630 Kawabata, Y., Akada, H., Shimatani, K.I., Nishihara, G.N., Kimura, H., Nishiumi, N. and
631 Domenici, P., 2023. Multiple preferred escape trajectories are explained by a geometric model
632 incorporating prey's turn and predator attack endpoint. *Elife*, 12, p.e77699.
633 <https://doi.org/10.7554/eLife.77699>

634 Jacobson, S.L., Bliss-Ketchum, L.L., de Rivera, C.E. and Smith, W.P., 2016. A behavior-based
635 framework for assessing barrier effects to wildlife from vehicle traffic volume. *Ecosphere*, 7(4),
636 p.e01345. <https://doi.org/10.1002/ecs2.1345>

637 Pakula, C.J., D'Angelo, G.J., Mowrer, A., Rhodes Jr, O.E. and DeVault, T.L., 2025. Caught in
638 headlights: captive white-tailed deer responses to variations in vehicle lighting during imminent
639 collision scenarios. *Applied Animal Behaviour Science*, 287, p.106652.
640 <https://doi.org/10.1016/j.applanim.2025.106652>

641 Provini, P., Tobalske, B.W., Crandell, K.E. and Abourachid, A., 2012. Transition from leg to
642 wing forces during take-off in birds. *Journal of Experimental Biology*, 215(23), pp.4115-4124.
643 <https://doi.org/10.1242/jeb.074484>

644 Pfeiffer, M.B., Blackwell, B.F., Seamans, T.W., Buckingham, B.N., Hoblet, J.L., Baumhardt,
645 P.E., DeVault, T.L. and Fernández-Juricic, E., 2021. Responses of turkey vultures to unmanned
646 aircraft systems vary by platform. *Scientific Reports*, 11(1), p.21655.
647 <https://doi.org/10.1038/s41598-021-01098-5>

648 Pfeiffer, M.B., Pullins, C.K., Beckerman, S.F., Hoblet, J.L. and Blackwell, B.F., 2023.
649 Investigating nocturnal UAS treatments in an applied context to prevent gulls from nesting on
650 rooftops. *Wildlife Society Bulletin*, 47(2), p.e1423. <https://doi.org/10.1002/wsb.1423>

651 Pfeiffer, M.B., Hoblet, J.L., Blackwell, B.F. and Fernández-Juricic, E., 2025. Preliminary effects
652 of UAS angle of approach on escape responses of a large-bodied raptor. *Drone Systems and*
653 *Applications*, 13, pp.1-9. <https://doi.org/10.1139/dsa-2024-0047>

654 R Core Team. 2024. R: A language and environment for statistical computing. R Foundation for
655 Statistical Computing. <https://www.R-project.org/>.

656 Rytwinski, T., Soanes, K., Jaeger, J.A., Fahrig, L., Findlay, C.S., Houlahan, J., Van Der Ree, R.
657 and van der Grift, E.A., 2016. How effective is road mitigation at reducing road-kill? A meta-
658 analysis. *PLoS one*, 11(11), p.e0166941. <https://doi.org/10.1371/journal.pone.0166941>

659 Schoeman, R.P., Patterson-Abrolat, C. and Plön, S., 2020. A global review of vessel collisions
660 with marine animals. *Frontiers in Marine Science*, 7,
661 p.292. <https://doi.org/10.3389/fmars.2020.00292>

662 Seiler, A. and Olsson, M., 2017. Wildlife deterrent methods for railways—an experimental study.
663 In *Railway ecology* (pp. 277-291). Cham: Springer International Publishing.
664 https://doi.org/10.1007/978-3-319-57496-7_17

665 Sibley, A., 2014. The Sibley guide to birds.

666 Silva, I. and Calabrese, J.M., 2024. Emerging opportunities for wildlife conservation with
667 sustainable autonomous transportation. *Frontiers in Ecology and the Environment*, 22(2),
668 p.e2697. <https://doi.org/10.1002/fee.2697>

669 Spanowicz, A.G., Teixeira, F.Z. and Jaeger, J.A., 2020. An adaptive plan for prioritizing road
670 sections for fencing to reduce animal mortality. *Conservation Biology*, 34(5), pp.1210-1220.
671 <https://doi.org/10.1111/cobi.13502>

672 Tjur, T., 2009. Coefficients of determination in logistic regression models—A new proposal: The
673 coefficient of discrimination. *The American Statistician*, 63(4), pp.366-372.
674 <https://doi.org/10.1198/tast.2009.08210>

675 Van der Ree, R., Gagnon, J.W. and Smith, D.J., 2015. Fencing: a valuable tool for reducing
676 wildlife-vehicle collisions and funnelling fauna to crossing structures. *Handbook of road*
677 *ecology*, pp.159-171. <https://doi.org/10.1002/9781118568170.ch20>

678 Vas, E., Lescroël, A., Duriez, O., Boguszewski, G. and Grémillet, D., 2015. Approaching birds
679 with drones: first experiments and ethical guidelines. *Biology letters*, 11(2).
680 <https://doi.org/10.1098/rsbl.2014.0754>

681 White, M.G., Duttonhefner, J.L. and Klug, P.E., 2025. Establishing protocols to apply repellents
682 while hazing crop pests: importance of habitat, flock size, and time on blackbird (*Icteridae*)
683 responses to a drone capable of spraying. *Wildlife Research*, 52(3), p.WR24066.
684 <https://doi.org/10.1071/WR24066>

685 Ydenberg, R.C. and Dill, L.M., 1986. The economics of fleeing from predators. In *Advances in*
686 *the Study of Behavior* (Vol. 16, pp. 229-249). Academic Press. [https://doi.org/10.1016/S0065-](https://doi.org/10.1016/S0065-3454(08)60192-8)
687 [3454\(08\)60192-8](https://doi.org/10.1016/S0065-3454(08)60192-8)

688